[1] M. Faraday, Phil. Trans. R. Soc. Lond. **121**, 299 (1831).
[2] P. Chen and K.-A. Wu, Phys. Rev. Lett. **85**, 3813 (2000).
[3] N. Périnet, D. Juric and L. S. Tuckerman, J. Fluid Mech. **635**, 1 (2009).
[4] F. H. Harlow and J. E. Welch, Phys. Fluids **8**, 2182 (1965).
[5] G. Tryggvason, B. Bunner, A. Esmaeeli, D. Juric, N. Al-Rawahi, W. Tauber, J. Han and Y.-J. Jan, J. Comput. Phys. **169**, 708 (2001).
[6] C. S. Peskin, J. Comput. Phys. **25**, 220 (1977).
[7] A. V. Kityk, J. Embs, V. V. Mekhonoshin and C. Wagner, Phys. Rev. E **72**, 036209 (2005).
[8] A. V. Kityk, J. Embs, V. V. Mekhonoshin and C. Wagner, Phys. Rev. E **79**, 029902 (2009).
[9] K. Kumar and L. S. Tuckerman, J. Fluid. Mech. **279**, 49 (1994).

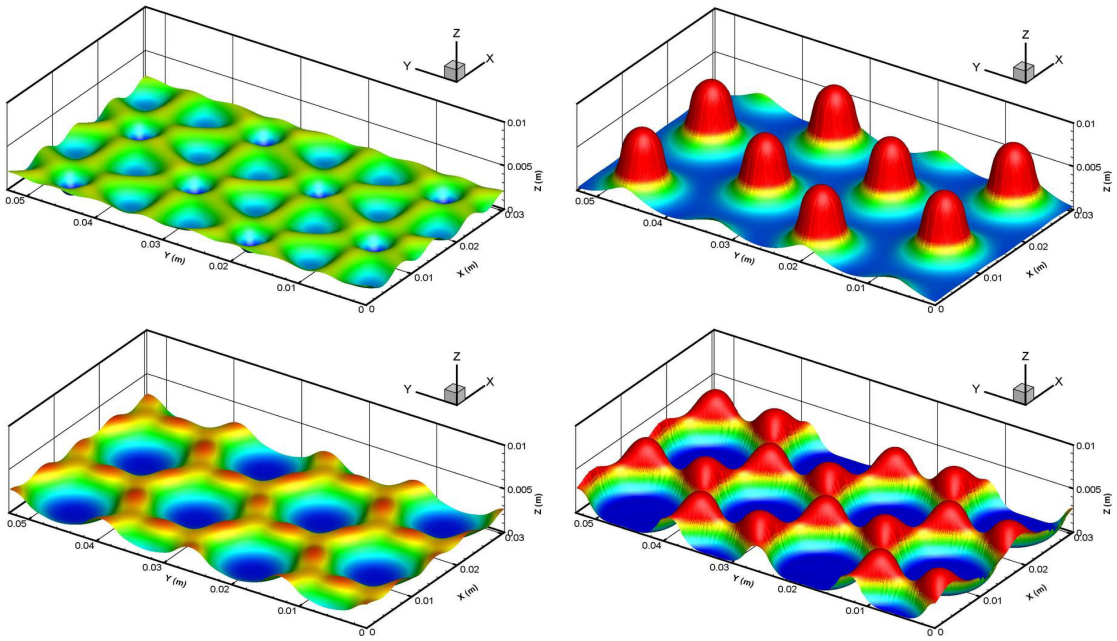

Figure 2: Visualizations of hexagonal interface over one subharmonic oscillation period. The size of the visualization domain is double that of the computational domain in each direction.

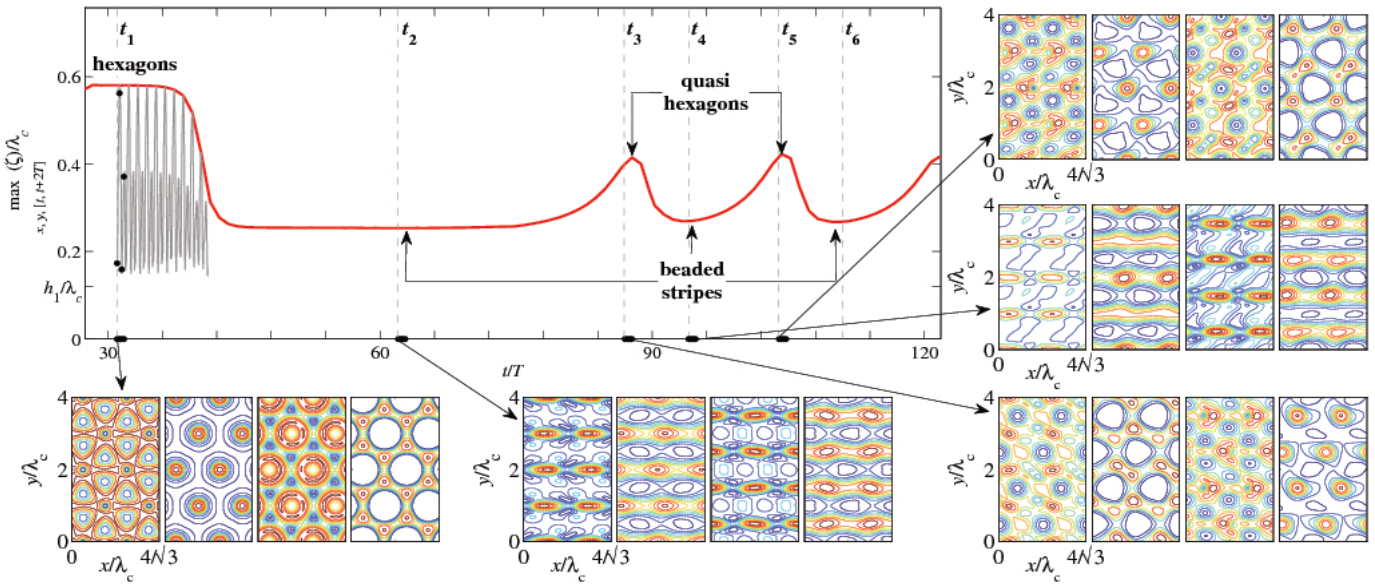

Figure 3: Maximum interface heights $\max_{x,y} \zeta(x,y,t)$ (rapidly oscillating curve) and $\max_{x,y,[t,t+T]} \zeta(x,y,t)$ (smooth curve). Surrounding visualizations show instantaneous contour plots of $\zeta(x,y,t)$. The size of the box has been doubled in each dimension. Visualizations shown at $t_i + j\,T/4$ for $j = 0, 1, 2, 3$, i.e. over one subharmonic period. The hexagonal patterns at time t_1 can be compared with the three-dimensional visualizations shown in figure 3. The pattern consists of beaded stripes at time t_2, quasi-hexagons at t_3 and t_5, and nonsymmetric beaded stripes at t_4 and t_6. Over the large white areas, the interface is very close to the bottom and almost flat. Patterns at t_3 and t_5, and at t_4 and t_6 are related by the spatio-temporal transformation (3).

RELAXATION PROCESSES IN COULOMB GLASSES

PROCESOS DE RELAJACIÓN EN VIDRIOS DE COULOMB

J. Bergli[a †] and Y. M. Galperin[a,b,c]

a) Department of Physics, University of Oslo, P.O.Box 1048 Blindern, N-0316 Oslo, Norway, jbergli@fys.uio.no[†]
b) A. F. Ioffe Physico-Technical Institute RAS, 194021 St. Petersburg, Russian Federation
c) Centre for Advanced Study at the Norwegian Academy of Science and L etters, 0271 Oslo, Norway
† corresponding author

Coulomb glasses are materials with electron states localized by the disorder under conditions of long-range interactions between their particles. One realization of a Coulomb glass is a doped semiconductor at low temperatures. Another example is granular metals. Coulomb glasses show complex dynamics typical for other complex systems: sluggish, non-exponential, relaxation of the conductance as well as aging and memory effects similar to those observed in structural glasses. We report dynamical Monte Carlo simulations of relaxation processes in a Coulomb glass. Both the relaxation to equilibrium following an initial temperature quench and during and after a driving by a strong current is studied. We see that out of equilibrium there is an effective electron temperature established on a short timescale, and this relaxes slowly to the bath temperature. We also study the response of the system to an external perturbation and observe how it relaxes after such a perturbation. Both from a random state and after a perturbation from equilibrium we find that the effective temperature relaxes logarithmically.

Los vidrios de Coulomb son materiales con estados electrónicos localizados debido al desorden, cuyas partículas poseen una interacción de Coulomb como, por ejemplo, un semiconductor dopado a baja temperatura, y un metal granular. Los vidrios de Coulomb muestran una dinámica típica de otros sistemas complejos: relajación lenta y no exponencial de la conductividad, y efectos de memoria similar a los observados en vidrios estructurales. En este trabajo, describimos simulaciones de Monte Carlo dinámicas de los procesos de relajación en vidrios de Coulomb. Estudiamos la relajación hacia el equilibrio, después de un enfriado rápido, y durante y después de una perturbación con una corriente eléctrica. Observamos que, fuera del equilibrio, se establece rápidamente una temperatura efectiva del sistema electrónico, y que éste relaja lentamente hacia la temperatura del baño. Estudiamos la respuesta del sistema a una perturbación externa, y la relajación después de la perturbación. Observamos que, en ambos casos, la temperatura efectiva muestra una relajación logarítmica.

PACS: Amorphous semiconductors glasses, 71.23.Cq; Disordered solids, 72.80.Ng; Hopping transport, 72.20.Ee

INTRODUCTION

At low temperatures, disordered systems with localized electrons (*e. g.*, located on dopants of compensated doped semiconductors or formed by Anderson localization in disordered conductors) conduct by phonon-assisted hopping. The theory of this process goes back to around 1970 and is well studied, see Ref. [1] for a review. In recent years, there has been increasing interest in the non-equilibrium dynamics of hopping systems. In particular, the glass-like behavior at low temperatures has been studied both experimentally [2] and theoretically [3]. In this work, we are interested in two features observed in the experiments. Firstly, it was observed that the conductivity relaxes logarithmically as a function of time after an initial quench or perturbation [2]. Secondly, if the system initially in equilibrium is perturbed by some change in external conditions (*e. g.*, temperature or electric field) for a time t_w called the waiting time, the relaxation back towards equilibrium of some quantity like the conductance $G(t,t_w)$ will depend both on t_w and the time t since the end of the perturbation. It is found in certain cases that the relaxation is in fact described by a function $G(t/t_w)$ of the ratio t/t_w. This behavior is called *simple aging* [2].

While simple aging is observed in a range of different systems, we are here particularly concerned with experiments on disordered InO films and porous silicon [2]. The relevant experimental facts can be summarized as follows: (i) After a quench from a high temperature state, the relaxation of conductance is close to logarithmic. (ii) The same is true after driving the system by a strong current. The rate of relaxation depends on the time the system was driven out of equilibrium (waiting time, t_w). When scaled with the waiting time, all curves collapse (simple aging). (iii) If the driving field is too strong, simple aging is no longer observed. (iv) If the waiting time is too long, simple aging is no longer observed.

One question which has been raised is whether the observed glassy behavior is an intrinsic feature of the electron system, or a result of some extrinsic mechanism like ionic rearrangement [4]. In this work, we address the *intrinsic* mechanism by performing dynamical Monte Carlo simulations of the standard lattice model of the electron glass. It is known [3] that during a quench from an initial random state an effective electron temperature,

T_{eff}, is quickly established, and that this temperature slowly relaxes to the bath temperature. We show that the electron temperature relaxes logarithmically over almost three decades in time and that the system demonstrates simple aging behavior in a stress aging protocol (driving by a strong electric current) similar to what is seen in the experiments. While this does not constitute a proof of the intrinsic origin of the glassy behavior, it shows that the model can display the observed behavior.

MODEL

We use the standard tight–binding Coulomb glass Hamiltonian [1],

$$H = \sum_i \epsilon_i n_i + \sum_{i<j} \frac{(n_i - K)(n_j - K)}{r_{ij}}, \quad (1)$$

K being the compensation ratio. We take e^2/d as our unit of energy where d is the lattice constant which we take as our unit of distance. The number of electrons is chosen to be half the number of sites so that K=1/2. ϵ_i are random site energies chosen uniformly in the interval [-U, U]. In the simulations presented here we used U = 1, which we know gives a well-developed Coulomb gap and the Efros-Shklovskii (ES) law for the conductance [5, 6]. The sites are arranged in two dimensions on a $L \times L$ lattice where in all cases we used L = 1000, which is sufficiently large to give a good estimate of the effective temperature in a single state without any averaging over a set of states. We implement cyclic boundary conditions in both directions.

To simulate the time evolution we used the dynamic Monte Carlo method introduced in Ref. [5], for a more detailed description, see Ref. [7]. In all our simulations we used a phonon temperature T = 0.05, which we know is well into the ES regime for variable range hopping. The graphs show the evolution over 10^8 jumps.

RELAXATION AND EFFECTIVE TEMPERATURE

Let us first relax from an initial random state and measure $T_{eff}(t)$. Shown in Fig. 1 are the energy (inset) and the effective temperature as functions of time. As we can see, the energy graph has almost stopped to decrease, indicating that we have almost reached equilibrium. The same is seen by the effective temperature, where T_{eff} = 0.054, close to the real temperature T = 0.05, in the final state. We see that the effective temperature, after some initial short time, logarithmically decreases in time for about two and a half orders of magnitude. The energy does not show this behavior (as discussed in Ref. [8], it is well fitted by a stretched exponential function). We then applied an electric field E = 0.1 (in units of e^2/d). Shown in Fig. 2 (left) is the energy per site as a function of time. The effective temperature as a function of time is shown in Fig. 2 (left, middle curve). Noting the difference in the timescales we conclude that the energy stabilizes at a new value much faster than the effective temperature.

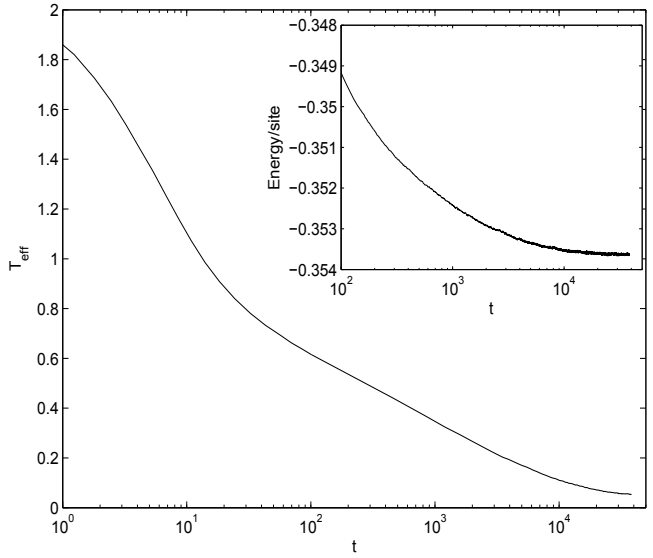

Figure 1: Effective temperature as function of time. The inset shows the energy as function of time.

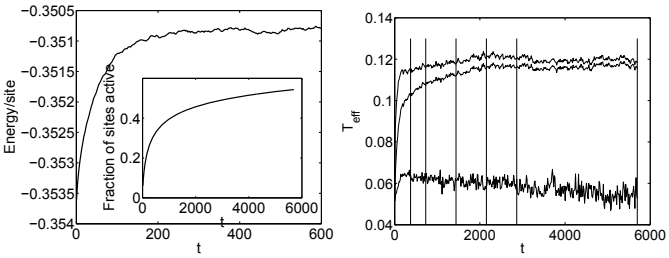

Figure 2: During driving with E = 0.01. Left: Energy as function of time. Inset: The fraction of sites involved in a jump as function of time. Right: Effective temperature as function of time. The curves are from top to bottom the temperature of the sites which were active, the temperature of all sites and the temperature of the sites which were not active. The vertical lines indicate the waiting times in the stress aging protocol (see Fig. 5).

We have also plotted the effective temperature taking into account only those sites which were involved in a jump, Fig. 2 (bottom, upper curve), and those which did not jump, Fig. 2 (bottom, lower curve). As we can see, the sites which are not involved in jumps are still at a temperature close to the phonon temperature. This is not a trivial statement, since the energies of the sites which are not involved in jumps also change due to the modified Coulomb interactions with the sites that jumped. Note that even at the latest time shown, new sites are still being involved, see Fig. 2 (top, inset), even if the energy and effective temperature are more or less stable. When driving with stronger fields we observed some heating also of the sites not involved in any jumps, while the distribution remained close to a Fermi distribution so that the concept of temperature sill has a meaning.

This is shown in Fig. 3. In particular we find it remarkable that also the sites never involved in transitions show a good fit to the Fermi distribution. Normally, we think of energy levels as fixed and occupation numbers changing dynamically in such a way as to maintain the Fermi distribution in the time averaged occupation probabilities. If the energy levels are shifted by

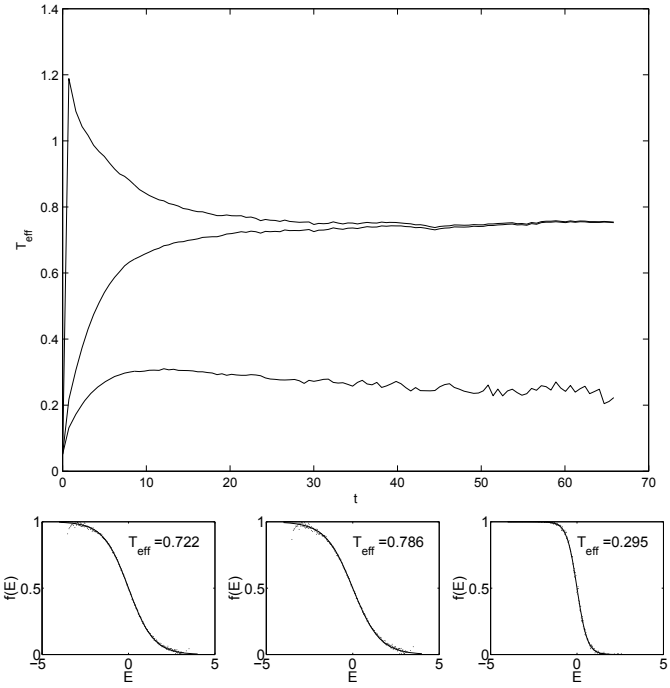

Figure 3: When driving with electric field $E = 1$. Top: T_{eff} as function of time. The curves are from top to bottom the temperature of the sites which were active, the temperature of all sites and the temperature of the sites which were not active. Bottom: Fitted Fermi functions at time $t = 19$. Left: All sites, Center: Sites which took part in a transition, Right: Sites which did not take part in a transition. The points are the data and the curve the fitted function.

some process, the transition rates also have to change, and the occupation numbers will adjust to the new energy level. In our case we have that the occupation numbers of the sites not involved in transitions are fixed, while their energies are pushed around by the interactions with the jumping sites. A natural guess would be that there is no correlation between the energy of a site before the driving starts (and hence the occupation probability of that site) and the shift it receives during driving. One would then guess that the initial Fermi distribution at the real phonon temperature would be scrambled during the driving, and that for the sites not involved in jumps we would not find a well defined Fermi function. The fact that this does not happen indicates that there is certain structure to the nature of the shifts of the energies, and would be an interesting point for further study.

The heating process can also be illustrated in another manner. In Fig. 4 is shown the single particle density of states (DOS) at different times after the start of the driving with $E = 0.1$ (the same as in Fig. 2). Curves for the total DOS as well as for the sites involved and not involved in jumps are shown. The total DOS shows initially a Coulomb gap corresponding to the real phonon temperature. This changes into the more smeared Coulomb gap of T_{eff} on a rather short time-scale. On times longer than this, the curves for jumped and non-jumped sites keep changing as more and more sites are involved in jumps. Thus, the state of the system keeps evolving for times much longer than the one needed for the overall Coulomb gap to adjust to the effective temperature.

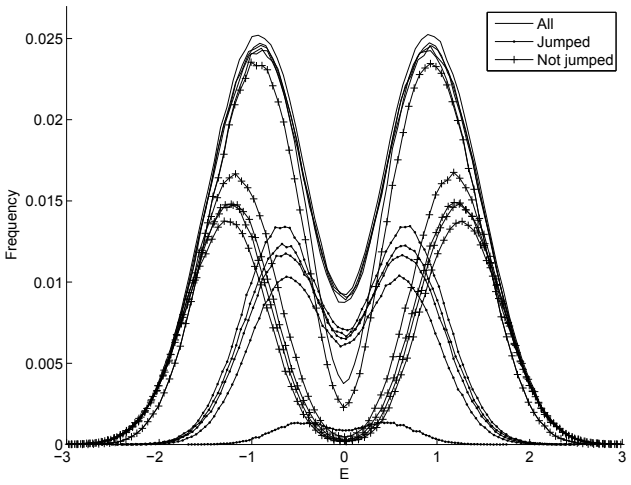

Figure 4: When driving with $E = 0.1$. The density of states at the times $t = 12.5$, 1426, 2851, 4275, and 5696. For the graphs of all sites and jumped sites the lower curves correspond to earlier times and the higher curves to later. For the not jumped sites lower curves correspond to longer times.

STRESS AGING

We now follow the stress aging protocol. This means applying a non-Ohmic field for a certain time t_w and then turning this field off. The heating process of Fig. 2 is exactly such a non-Ohmic driving, and we need only start simulations with zero fields at different points along this curve. We have chosen six t_w, which correspond to the points marked on Fig. 2 with vertical lines.

Figure 5 shows the effective temperature as function of t/t_w after the end of the driving period. Note that the time dependence of the energy is very similar in all cases as shown in Fig. 5 (inset). From Fig. 5 we conclude that there is a logarithmic relaxation of the effective temperature after a driving by a non-Ohmic field just as in the case of relaxation from a random initial state (Fig. 1). Furthermore, we see that the curves for different t_w collapse when time is scaled with t_w when t_w is smaller than some critical value $t_w^{(c)} \approx 2500$. The curve for $t_w = 2865$ seems to lie a little to the left of the collapse curve, and for $t_w = 5696$ this tendency is clear. The collapse of the curves for short t_w is similar to what is observed in the experiments both on indium oxide films and porous silicon [2]. In the case of porous silicon, also the departure from the simple aging at longer waiting times was observed, while sufficiently long times were never reached in the case of indium oxide.

If we compare to Fig. 2 (right) we see that the critical value t_w corresponds to the time where the effective temperature stabilizes. Comparing to Fig. 2 (left) we see that this is a time much longer than the one, which is needed for the energy to stabilize.

We also repeated the stress aging protocol at different driving fields, $E = 0.05$, 0.2, 0.5 and 1. Note that to be in the Ohmic regime we should have $E \lesssim T/10$, so all the fields are well outside of this. For $E = 0.05$ the effective temperature as